Geophysical Research Letters

RESEARCH LETTER
10.1029/2018GL079391

Key Points:
- We analyze the sublimation of contrail ice crystals in the aircraft wake vortex regime
- Wake-average ice numbers increase with soot emissions despite significant sublimation losses
- Inhomogeneous vertical distributions of ice numbers affect processes controlling contrail life cycles

Supporting Information:
- Supporting Information S1

Correspondence to:
B. Kärcher,
bernd.kaercher@dlr.de

Citation:
Kärcher, B., Kleine, J., Sauer, D., & Voigt, C. (2018). Contrail formation: Analysis of sublimation mechanisms. *Geophysical Research Letters*, *45*. https://doi.org/10.1029/2018GL079391

Received 28 JUN 2018
Accepted 23 AUG 2018
Accepted article online 29 AUG 2018

©2018. American Geophysical Union. All Rights Reserved.

Contrail Formation: Analysis of Sublimation Mechanisms

B. Kärcher[1], J. Kleine[1,2], D. Sauer[1], and C. Voigt[1,2]

[1]Institut für Physik der Atmosphäre, Deutsches Zentrum für Luft- und Raumfahrt, Oberpfaffenhofen, Germany, [2]Institut für Physik der Atmosphäre, Johannes Gutenberg Universität Mainz, Mainz, Germany

Abstract We study losses of ice crystals in a persistent, soot-rich contrail in the wake behind a medium-sized aircraft at cruise. Constraining a model covering ice nucleation, growth, and sublimation phases with an aircraft data set, we track the sublimation history over 2 min of contrail age and relate ice crystal numbers to the number of soot particles emitted by the aircraft engines. We analyze the observed vertical distribution of ice numbers, estimating an exponential scale height in the range 50–100 m and wake-averaged ice numbers (1.3–1.7) $\times$ 10^{15} $(\text{kg-fuel})^{-1}$ after sublimation, removing 60% of the ice crystals that originally nucleated on emitted soot particles. We define soot emission- and ice supersaturation-dependent contrail depths, affecting estimates of horizontal spreading rates of contrails. Our findings have ramifications for the representation of long-lived contrails in global models.

Plain Language Summary Contrails are climate-forcing agents, but their overall climatic effect is difficult to quantify. Airborne measurements quantify properties of the initially line-shaped ice clouds forming behind cruising jet aircraft. Exploring the formation stage of contrails reveals something about their properties and enables us to predict how they evolve in the atmosphere. We elucidate processes in a contrail that remove within few minutes more than half of the ice crystals generated from the engine emissions. Ice crystal number in, and vertical extension of, young contrails are fundamental determinants of processes governing their life cycle and climate impact. Our results highlight the need for focused observational studies and pave the way for improvements in the representation of contrails and the clouds evolving from them in climate models.

1. Introduction

Contrail cirrus clouds originating from jet aircraft at cruise perturb natural cirrus and radiative fluxes. Characterization of long-lived contrails in their formation stage is a key step in assessing their impact on climate and aids efforts to reduce this impact in the context of curbing anthropogenic global warming (Kärcher, 2018).

The aircraft-dominated contrail formation stage lasts 5–10 min and comprises jet, vortex, and dissipation regimes. In the jet regime (<10 s), a large number of small ice crystals nucleate in cooling exhaust plumes that emanate from jet engines and grow by uptake of water vapor. In the subsequent vortex regime within few minutes of contrail age, a significant fraction of plume air descends below the flight level (hereinafter primary wake, pw). The associated adiabatic warming forces contrail ice crystals captured in pw to sublimate, while those present in the plume around the flight level (secondary wake, sw) grow by deposition of water vapor in ice-supersaturated ambient conditions. In the dissipation regime, ice crystals mix in the collapsing and decaying wakes, setting initial depth and total number and mean size of ice crystals in long-lived contrails. In sum, this demonstrates that water vapor emissions and contrail ice crystals cannot be simply viewed as passive exhaust plume tracers; instead, they are strongly affected by microphysical processes that are in turn driven by plume and wake dynamics. These processes must be predicted with confidence as functions of engine emissions, aircraft, and atmospheric variables to initialize contrails in models with low resolution by way of parameterization.

Modeling tools with various degrees of complexity have been developed to study formation stage processes, ranging from microphysical parcel models to fluid-dynamical large-eddy simulations (LES; see Paoli & Shariff, 2016, and references therein). Detailed model validation is hampered primarily by a lack of contrail measurements in ice-supersaturated conditions. Here we focus on the vortex regime seeking a quantitative explanation of observed ice crystal losses. We thereby validate a microphysical-dynamical contrail model

(Kärcher & Voigt, 2017; Kärcher et al., 2015) by a process-based analysis of aircraft measurements taken in a freshly generated, persistent contrail (Kleine et al., 2018).

Evidence for a contribution of aircraft-emitted soot particles to contrail ice crystal formation has been reported based on measurements in the jet regime of a short-lived contrail (Figure 3 in Schröder et al., 1998). Ice crystal sublimation has been observed, but not quantified, in the vortex regime of short-lived contrails (Figure 2 in Schumann et al., 2013). Here we extend these studies to a low-temperature contrail that formed in ice-supersaturated air allowing it to survive the vortex regime. We outline experimental information relevant for our study and recall salient features of our model in section 2, develop the model analysis in section 3, and conclude our study in section 4.

2. Prerequisites

2.1. Data Set (ECLIF Flight 10; 7 October 2015)

In situ measurements were performed within the DLR project ECLIF (Emission and climate impact of alternative fuel). Contrails were generated behind the Advanced Technology Research Aircraft (ATRA) research aircraft, a modified Airbus A 320, equipped with two jet engines. One project goal was to study links between contrail ice crystals and aircraft-emitted soot particles depending on fuel type and ambient conditions. Ambient pressure and temperature at the ATRA flight level were $p = 238$ hPa and $T = 215.5$ K, respectively. Air in the contrail environment was supersaturated with respect to ice, with associated relative humidities in the range RHI = 115–125%. During flight 10, the ATRA burned conventional aviation fuel. Given the high soot particle number emission indices, contrail ice crystals mainly originate from emitted soot particles.

The ATRA aircraft (wingspan $B = 34.1$ m, fuel flow $\dot{m}_f = 0.33$ kg-fuel/s per engine) weighed 49,600 kg and cruised at a speed $V = 188$ m/s. We estimate a mean vortex sinking speed, $w = 1.5$ m/s (Equation (A3) in Unterstrasser, 2016) and a vertical extension (depth) of the primary wake, $z_{\mathrm{pw}} = 155$ m (Equation (2) in Schumann et al., 2013). The altitude difference, z, between the flight level of the source aircraft and the vertical position of the probing aircraft within the wake was determined using the Global Positioning System (GPS) with an estimated accuracy of ± 15 m depending on the distance behind the source aircraft (≈7–25 km or contrail ages 39–132 s).

2.2. Model Approach

Our approach rests upon an air parcel methodology that includes effects of turbulent entrainment of air surrounding the jet contrail, designed to model total ice crystal numbers and mean sizes after the sublimation phase. It is not capable of representing spatial variability within aircraft wakes as is possible with LES models. This does not limit its suitability for the present analysis. We include information on vertical ice number variability—important for estimates of wake-averaged total ice numbers—into the model framework. Advantages of this approach are that interdependencies among physical variables are explicitly identifiable in analytical relationships and that those variables can be varied parametrically with virtually no computational effort.

To analyze the aircraft data set, the output of the nucleation parameterization (Kärcher et al., 2015) is used to calculate, in the jet regime, the apparent total ice crystal emission index (number concentration corrected for plume dilution effects), AEI; mean volume radius, r, of contrail ice crystals; and bulk plume supersaturation over ice, s, as a function of the soot emission index, EI_s, and other parameters. In the absence of data, emitted soot particles are distributed lognormally with a geometric mean radius of 15 nm and standard deviation 1.6 (Moore et al., 2017) and are associated with a soluble volume fraction of 1% (Petzold et al., 2005). While these parameters must be known with confidence in contrails forming near the thermodynamic formation threshold temperature (in our case, $\Theta \simeq 225$ K), the results presented here are insensitive to these choices. Prior to ice formation, water activation of emitted soot particles in the cooling plumes generates water droplets that freeze homogeneously. Other parameters affecting contrail ice nucleation include the overall propulsion efficiency (0.3) and the ratio of water vapor mass emission index and specific heat of fuel combustion (0.0285 kg/MJ for kerosene), resulting in a slope of the jet plume mixing line, 1.56 hPa/K. The nucleation efficiency is defined by $f_\star = \mathrm{AEI}_\star/\mathrm{EI}_s$. Here $\mathrm{AEI}_\star$ is the nucleated ice number that stays constant in the jet regime of persistent contrails, while r and s change over time. As the current measurements were performed in soot-rich conditions about 9.5 K below Θ, the nucleation efficiency is close to unity ($f_\star = 0.96$).

The evolution of ice crystals is split up into upper (sw) and lower (pw) wake components, as both dynamical and microphysical processes modifying ice crystals evolve differently in different wake regions. We calculate

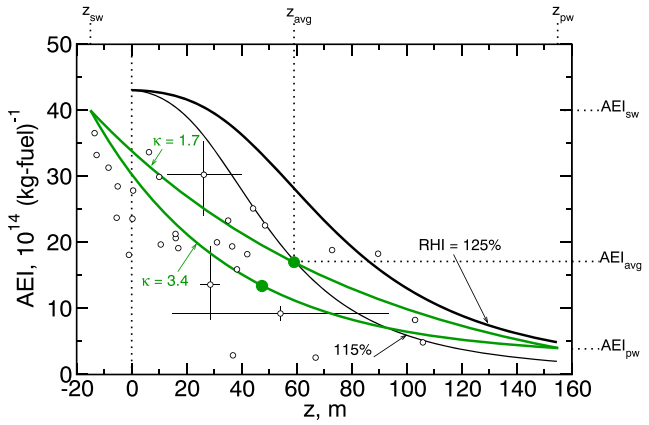

Figure 1. Apparent contrail ice crystal emission index, AEI, versus vertical wake position, z, above and below the flight level ($z = 0$) of the contrailing aircraft from aircraft measurements (circles) and from the model analysis (curves). Positive (negative) positions extend into the primary (secondary) wake up to z_{pw} (z_{sw}) approaching AEI_{pw} (AEI_{sw}). AEI data points represent averages over various z ranges and positions behind the contrailing aircraft. The data points show considerable case-to-case variability in terms of their uncertainty, as indicated by three examples. The model tracks the vortex regime history of sublimation losses affecting peak AEI values in the primary wake using jet regime results from a nucleation model. Black curves are model results designed to capture AEI maxima, indicating the sensitivity to ambient ice supersaturation. Green curves are exponentials with scale heights $\mathcal{H} = 100\,(50)$ m, or $\kappa = 1.7\,(3.4)$, capturing the full variability in AEI and therefore used to estimate AEI_{avg}. Green circles mark the wake positions, $z_{avg} = 59\,(47)$ m, where these averages are reached. They may be used to define characteristic contrail (ice crystal distribution) depths $h = z_{avg} - z_{sw} \approx 74\,(62)$ m, significantly smaller than the geometrical wake depth, $H = z_{pw} - z_{sw} = 170$ m. RHI = relative humidity.

the sublimation history in pw based on AEI, r, and s for given EI_s at $t = 10$ s (Kärcher & Voigt, 2017). This solution describes the conditions of ice supersaturation and total number and mean size of ice crystals in contrail jet plumes in a physically self-consistent manner. (Contrary to water vapor, contrail ice crystals are not emitted; turbulent mixing establishes ambient relative humidity levels in the aging jet plume.) The model yields a mean contrail ice crystal radius of 0.43 μm at $t = 10$ s, in line with the data suggesting 0.45 ± 0.1 μm at 1–4 s. The mean size of ice crystals in soot-rich contrails does not increase significantly in the formation stage after deposition of the initially highly ice-supersaturated exhaust water vapor, since the high ice crystal number concentration forces the plume to stay very close to ice saturation counteracting the mixing tendency. The Kelvin effect affects the rate of ice crystal sublimation in pw, especially in soot-rich contrails. As sublimation depends on particle size, we assume a lognormal ice crystal size distribution with a geometric standard deviation, σ, not predicted by the model. We use $\sigma = 1.5$, approximately representing the size distribution in the peak regions around the mean size as measured in upper parts of the vortex wake that are only weakly affected by sublimation. The temporal evolution of ice crystal size distributions in a primary aircraft wake is shown in Figure S1 in the supporting information in Kärcher and Voigt (2017), showing that σ increases over time due to an enhanced abundance of small, sublimating particles.

The factor f_{pw} denotes the fraction of ice crystals in pw (relative to $AEI_\star$) that escape full sublimation. According to the above, the nucleation phase affects f_{pw} via the plume variables $\{f_\star, r, s, \sigma\}$ for given EI_s and jet engine/fuel properties. Aircraft type and ambient stratification enter f_{pw} via the full geometrical wake depth, H. Descending pw air warms adiabatically along the dry adiabate ($\Gamma = 9.8$ K/km), leading to a warming tendency, $w\,\Gamma \simeq 0.9$ K/min, forcing the small ice crystals in soot-rich contrails to sublimate almost instantly. Hence, AEI decreases in pw according to $f_{pw}(z) \cdot AEI_\star$. The vortex descent past $t = 10$ s lasts about $z_{pw}/w = 1.7$ min, causing a final $z_{pw}\,\Gamma \simeq 1.5$ K warming of air in pw relative to the flight level ($z = 0$). The GPS altitude difference between the flight level and the location of the probing aircraft is related to the time elapsed since the start of the pw descent via $z = w \cdot (t - 10\,\text{s})$. The secondary wake detrains from the downward-moving primary vortices extending slightly above the flight level. We therefore expect the uppermost wake part to contain most ice crystals.

3. Analysis

3.1. Sublimation Losses

Figure 1 shows AEI versus z over ≈2 min of contrail age, during which the wake vortex pair descends a distance z_{pw}, at which point our model estimates the minimum ice number in pw after sublimation: $AEI_{pw} = f_{pw}(z_{pw})AEI_\star$. Losses decrease upward toward the approximate sw depth $|z_{sw}|$, where ice numbers approach $AEI_{sw} = AEI_\star = f_\star EI_s$, as expected, with $EI_s = (4\text{–}5) \times 10^{15}$ (kg-fuel)$^{-1}$ (Kleine et al., 2018). In this case, the sensitivity of $f_\star$ to RHI, EI_s, and to properties of the soot particle size distribution is small.

Data-model comparison is hampered by the fact that data points attributed to a single vertical level represent in reality averages over a range of z values (horizontal lines) belonging to different contrail ages in the model. Experimental sources of uncertainty for AEI (vertical lines) include plume dilution factors, statistical counting errors and empirical corrections accounting for undersampling of ice crystals. Uncertainty due to the latter is quantified only to a degree and is therefore not included in Figure 1.

The black curves are model results based on $EI_s = 4.5 \times 10^{15}$ (kg-fuel)$^{-1}$ for upper and lower limit RHI values. The resulting changes in final ice numbers, $AEI_{pw} = (2\text{–}5) \times 10^{14}$ (kg-fuel)$^{-1}$, are moderate for the soot-rich contrail. These model curves bracket the data points that most likely belong to the pw core region. Lowering EI_s twofold does not significantly change AEI_{pw} values (not shown) due to the buffering effect of sublimation.

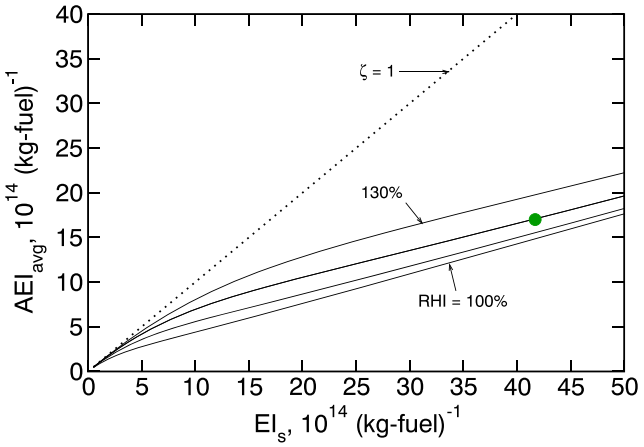

Figure 2. Wake-averaged apparent contrail ice crystal emission index, AEI_{avg}, versus soot emission index, EI_s, from the parameterization using $\kappa = 1.7$ for selected ambient RHI values. RHI increases in 10% increments from ice saturation (100%) onward. Results are taken at the end of the vortex descent at $z = z_{pw}$; the sensitivity to this choice is small, since the sublimation efficiency approaches a constant value; see Figure 1. The dotted line shows the soot-ice relationship if ice nucleation was perfectly efficient and sublimation did not occur. The green circle marks our best estimate value for AEI_{avg}, based on $\kappa = 1.7$. RHI = relative humidity.

We estimate the final sublimation-induced ice crystal losses to be $1 - f_{pw}(z_{pw}) = 0.87$. As the black model curves do not accurately represent AEI within the transition region between sw and pw around the dotted line at $z = 0$ (section 2.2), the AEI(z) data are better fitted by constrained exponentials (green curves), which we use for further analysis.

3.2. Wake-Averaged Ice Numbers and Contrail Depth

We have investigated how sublimation losses affect nucleated AEI in the lower wake region toward z_{pw}. Together with contrail depth and width, wake-averaged ice numbers, AEI_{avg}, are needed to initialize global model simulations of contrail cirrus evolution. Average ice numbers may be defined as $AEI_{avg} = (1/H)\int_{z_{sw}}^{z_{pw}} AEI(z)dz$. In our model, this integral is approximated by $AEI_{avg} = (1-\eta)AEI_{pw} + \eta AEI_{sw}$ (Kärcher & Voigt, 2017). It is important to have a robust means to estimate the fractional weight, η, which is determined by complex fluid-dynamical processes (Figure 8 in Gerz et al., 1998). In the supporting information, we evaluate the integral by using an exponential profile that allows us to compute AEI_{avg} analytically. We constrain the exponential by $\{z_{sw}, AEI_{sw}; z_{pw}, AEI_{pw}\}$ and use the AEI scale height as a parameter to fit the specific observations. Due to the flexibility of matching a variety of conceivable vertical AEI profiles as displayed in Figure S1, we expect exponential functions constrained in this way to fit other observational data sets as well.

We combine experimental information—in the form of AEI(z)—into our model framework and constrain η by equating the two above definitions of AEI_{avg}, leading to $\eta = 1+\kappa^{-1}-(1-e^{-\kappa})^{-1}$, thereby introducing the dimensionless contrail depth $\kappa = H/\mathcal{H}$. This relationship is convenient, because $\mathcal{H}$ and therefore $AEI(z) \propto \exp(-z/\mathcal{H})$ can be directly related to the aircraft measurements. The parameter κ depends on type of aircraft and rate of sublimation; the latter is strongly affected by $AEI_\star$, hence EI_s: While for $\kappa > 1$ ice crystal numbers decrease notably already in the upper portions of the wake (see Figure S1 in the supporting information), ice crystals are lost gradually over H if $\kappa < 1$. Visual inspection of contrails indeed suggests variability in the vertical distribution of ice crystals in the vortex regime (Figure 1 in Jeßberger et al., 2013), hence in κ.

Choosing $\mathcal{H} = 100\,(50)$ m gives $\kappa = 1.7\,(3.4)$ and $\eta = 0.37\,(0.26)$, resulting in the green curves shown in Figure 1. This yields our best estimates $AEI_{avg} = 1.7\,(1.3) \times 10^{15}$ (kg-fuel)$^{-1}$ using $AEI_{sw} = 4 \times 10^{15}$ (kg-fuel)$^{-1}$, equivalent to $EI_s \simeq 4.2{\times}10^{15}$ (kg-fuel)$^{-1}$, and $AEI_{pw} = 4{\times}10^{14}$ (kg-fuel)$^{-1}$, the model result within the observed RHI range. With $f_{pw}(z_{pw}) = 0.13$, this corresponds to an overall ice formation efficiency, $\zeta = AEI_{avg}/EI_s = f_\star[(1-\eta)f_{pw} + \eta] = 0.43\,(0.34)$ (Equation (16) in Kärcher & Voigt, 2017), or $\zeta/f_\star = 0.45\,(0.35)$ without accounting for incomplete nucleation of soot particles. This means that at $t = 10\,\text{s} + z_{pw}/w = 1.9$ min, sublimation removes on average about 60% of the ice crystals that originally nucleated on the emitted soot particles.

Figure 2 shows the dependence of AEI_{avg} on EI_s and RHI estimated with our model based on the present observations. In conditions of reduced ice formation efficiency (region $\zeta < 1$ below the dotted line) for $EI_s > (5\text{–}15) \times 10^{14}$ (kg-fuel)$^{-1}$, the EI_s dependence is linear and the RHI dependence is moderate. For the same reduction in EI_s, larger reductions in AEI_{avg} are possible for $EI_s < (5\text{–}15) \times 10^{14}$ (kg-fuel)$^{-1}$, as the slope $(\partial AEI_{avg}/\partial EI_s)_{RHI}$ increases toward low soot emissions due to diminishing sublimation losses.

We infer total ice crystal number concentrations per unit volume of air in the contrail at 1.9 min via $AEI \cdot 2\dot{m}_f/(VBH)$, yielding values up to 800–1,000 cm^{-3} that are roughly in line with the observations (Kleine et al., 2018). Wake dissipation and mixing immediately following the sublimation phase lowers number concentrations over time. LES results show that mixing may not be strong enough to redistribute ice numbers homogeneously in the wake within 5 min of contrail age (Figure 4 in Gerz et al., 1998).

4. Summary and Conclusions

We know that the number of ice crystals in young contrails can be reduced by aircraft wake-induced sublimation even in ambient air that is supersaturated with respect to ice. Here we analyze a unique data set of a contrail that formed behind a medium-sized aircraft in ice-supersaturated ambient conditions, ensuring

persistence and a large radiative forcing potential. In particular, we study in unprecedented detail the reduction in nucleated ice crystal number due to sublimation as it unfolds in the wake vortex regime.

Deriving accurate wake-average total ice crystal ice numbers from aircraft measurements alone is not straightforward due to the difficulty to sample aircraft wakes homogeneously. By constraining a parametric contrail model with aircraft observations, we explain for the first time the full sublimation history based on the state of the contrail in the late jet regime, quantify associated ice crystal losses toward the end of the vortex regime, and relate those losses to soot particle number emissions. We make use of the observed vertical profile of ice crystal number to infer wake-average ice number and associated contrail depth after sublimation. Despite significant ice crystal losses, average ice numbers increase monotonically with soot particle number emissions in soot-rich contrails.

Uncertainties in aircraft measurements of high ice crystal number concentrations in jet regime contrails prevent direct verification of nucleated ice numbers in contrails before significant sublimation occurs. Our analysis provides unequivocal, albeit indirect, proof of existence of high nucleated ice numbers as predicted by the nucleation model. If the nucleated AEI were substantially lower than modeled, then the predicted sublimation losses in the primary wake would be lower than observed.

Contrail parameterizations used in global models are based on two-moment microphysical schemes and represent large, inhomogeneous cloud fields by bulk ice crystal number and mass. Horizontal spreading rates of contrails, hence areal contrail coverage, increase due to wind shear in proportion to the contrail's vertical extension. Our combined nucleation/sublimation model, augmented by dilution of ice crystal numbers due to mixing right after the vortex regime, is useful for initializing such parameterizations. In view of the observed vertical ice number inhomogeneity in aircraft wakes, we raise the issue of a proper definition of contrail depth used in spreading calculations. Initial contrail depths and average ice numbers depend on soot emissions and ambient ice supersaturation. For instance, we envisage cases where strong sublimation—favored by high soot particle numbers and low ambient ice supersaturation—basically depletes most nucleated ice crystals in pw, so that only a shallow, upper contrail layer with high ice numbers remains. Such cases may frequently occur in cruise conditions behind heavy aircraft, where large wake depths and vortex sinking speeds cause rapid sublimation tendencies.

The magnitude of sublimation losses, hence, ice crystal numbers in contrails, differ for different types of aircraft, engine/fuel properties, and atmospheric conditions. Therefore, we see the need to conduct similar measurements for larger aircraft over a wide range of soot emissions and to carry out additional LES studies using high-resolution observational data sets for process evaluation and validation. Future contrail measurements should attempt to sample vertical profiles at the end of the formation stage (after wake dissipation), including more extensive characterization of upper wake layers. Moreover, experimental information about size distributions and chemical composition of aircraft-emitted soot particles is needed, as ice numbers in threshold contrails (in many cases forming near 225 K at cruise altitudes) are quite sensitive to soot particle number, size, and hygroscopicity. This is particularly important in efforts to quantify reductions in soot particle number emissions from alternative aviation fuels or propulsion technologies and to improve aircraft soot emission inventories. Making use of such data, future contrail parameterizations should cover the full suite of formation stage processes. More observations are needed to validate model predictions of near-threshold contrails frequently forming in low latitudes to better judge their overall climatic effects.

Acknowledgments
This study was supported by the DLR project ECLIF. C. V. acknowledges funding by the Helmholtz Society under contract W2/W3-60. The data set analyzed here is available at https://halo-db.pa.op.dlr.de.

References

Gerz, T., Dürbeck, T., & Konopka, P. (1998). Transport and effective diffusion of aircraft emissions. *Journal of Geophysical Research*, *103*, 25,905–25,913.

Jeßberger, P., Voigt, C., Schumann, U., Sölch, I., Schlager, H., Kaufmann, S., et al. (2013). Aircraft type influence on contrail properties. *Atmospheric Chemistry and Physics*, *13*, 11,965–11,984.

Kärcher, B. (2018). Formation and radiative forcing of contrail cirrus. *Nature Communications*, *9*, 1824. https://doi.org/10.1038/s-41467-018-04068-0

Kärcher, B., Burkhardt, U., Bier, A., Bock, L., & Ford, I. J. (2015). The microphysical pathway to contrail formation. *Journal of Geophysical Research: Atmospheres*, *120*, 7893–7927. https://doi.org/10.1002/2015JD023491

Kärcher, B., & Voigt, C. (2017). Susceptibility of contrail ice crystal numbers to aircraft soot emissions. *Geophysical Research Letters*, *44*, 8037–8046. https://doi.org/10.1002/2017GL074949

Kleine, J., Voigt, C., Sauer, D., Schlager, H., Scheiber, M., Jurkat-Witschas, T., et al. (2018). In situ observations of ice particle losses in a young contrail. *Geophysical Research Letters*, *45*. https://doi.org/10.1029/2018GL079390

Moore, R. H., Thornhill, K. L., Weinzierl, B., Sauer, D., D'Ascoli, E., Kim, J., et al. (2017). Biofuel blending reduces particle emissions from aircraft engines at cruise conditions. *Nature*, *543*, 411–415. https://doi.org/10.1038/nature21420

Paoli, R., & Shariff, K. (2016). Contrail modeling and simulation. *Annual Review of Fluid Mechanics*, *48*, 393–427.
Petzold, A., Gysel, M., Vancassel, X., Hitzenberger, R., Puxbaum, H., Vrochticky, S., et al. (2005). On the effects of organic matter and sulphur-containing compounds on the CCN activation of combustion particles. *Atmospheric Chemistry and Physics*, *5*, 3187–3203.
Schröder, F. P., Kärcher, B., Petzold, A., Baumann, R., Busen, R., Hoell, C., et al. (1998). Ultrafine aerosol particles in aircraft plumes: In situ observations. *Geophysical Research Letters*, *25*, 2789–2792.
Schumann, U., Jeß berger, P., & Voigt, C. (2013). Contrail ice particles in aircraft wakes and their climatic importance. *Geophysical Research Letters*, *40*, 2867–2872. https://doi.org/10.1002/grl.50539
Unterstrasser, S. (2016). Properties of young contrails—A parametrisation based on large-eddy simulations. *Atmospheric Chemistry and Physics*, *16*, 2059–2082.